

# A frustrated nanomechanical device powered by the lateral Casimir force

MirFaez Miri\*

*Institute for Advanced Studies in Basic Sciences (IASBS), P. O. Box 45195-1159, Zanjan 45195, Iran*

Ramin Golestanian†

*Department of Physics and Astronomy, University of Sheffield, Sheffield S3 7RH, UK*

(Dated: February 28, 2008)

The coupling between corrugated surfaces due to the lateral Casimir force is employed to propose a nanoscale mechanical device composed of two racks and a pinion. The noncontact nature of the interaction allows for the system to be made frustrated by choosing the two racks to move in the same direction and forcing the pinion to choose between two opposite directions. This leads to a rich and sensitive phase behavior, which makes the device potentially useful as a mechanical *sensor* or *amplifier*. The device could also be used to make a mechanical *clock* signal of tunable frequency.

PACS numbers: 07.10.Cm, 42.50.Lc, 46.55.+d, 85.85.+j

With the ongoing miniaturization of the mechanical systems, managing the tribological interactions at small length scales is proving to be one of the most significant challenges ahead of us.<sup>1</sup> A specific area of concern is the durability of mechanical parts that have fine geometrical features and come in contact with one another, as they can wear out very quickly.<sup>2</sup> Another important issue is to avoid the stiction of the mechanical components in small machines.<sup>3,4,5</sup> These problems suggest that we should try and develop design strategies for small scale mechanical systems that do not rely heavily on physical contact between machine parts.

In recent years, the Casimir force<sup>6,7</sup>—that originates from the quantum fluctuations of the electromagnetic vacuum—has emerged as a surprise candidate for non-contact actuation of mechanical devices.<sup>8,9</sup> Although the standard normal Casimir force in the original parallel-plate geometry might offer limited applicability because it is susceptible to instabilities,<sup>3</sup> it is possible to take advantage of geometrical features such as corrugations on the surfaces and produce a lateral component to the Casimir force<sup>10</sup> that can be used in stable mechanical force transduction.<sup>11</sup>

The lateral Casimir force between corrugated surfaces has been recently used as a basis for designing noncontact mechanical devices. It has been shown that the lateral Casimir grip can hold up relatively high velocities in a rack-and-pinion device<sup>12</sup> and that such a device can have a rich dynamical phase behavior. This includes, for example, the possibility of spontaneous symmetry breaking in the form of the rectification of lateral vibrations.<sup>13</sup> It has also been shown that normal undulations can be rectified into net lateral motion in such devices using a ratchet-like mechanism.<sup>14</sup>

Here, we propose a device made with two racks and a pinion as shown schematically in Fig. 1. The racks are set to move in the same direction, which renders the dynamics of the pinion frustrated due to the competing nonlinear couplings. The combination of frustration and nonlinearity could readily drive the system towards erratic

behavior and chaos, which would be an undesirable characteristic for a mechanical device. Therefore, we choose to consider the case of a heavily damped system, so that inertia can be neglected, which helps avoid the possibility of chaotic behavior. We probe the motion of the pinion in the different parts of the parameter space corresponding to the two rack velocities and the two amplitudes of the lateral Casimir force coupling that depend on the geometrical characteristics of the setup (see Fig. 1). We find that the system could have five distinct behaviors: (i) the pinion could be locked with either rack-1 or rack-2, (ii) the pinion could move along with either rack-1 or rack-2 but with a lower average velocity, and (iii) the pinion could oscillate back and forth without choosing to go with either of the racks. The oscillatory regime could be used to generate a clock signal of tunable frequency.

The corrugated surface of the pinion experiences a lateral Casimir force of the form<sup>10</sup>  $F_{\text{lateral}} =$

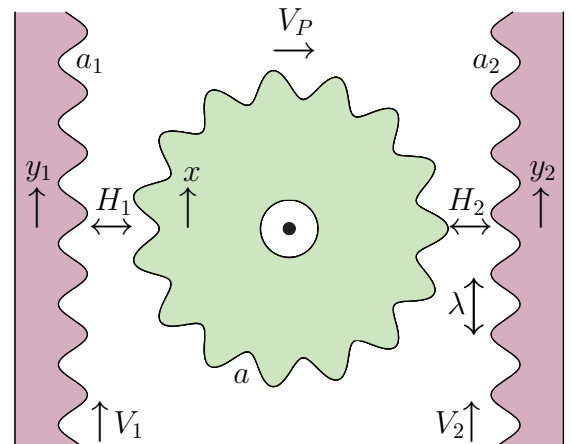


FIG. 1: (Color online). The schematics of the rack-pinion-rack device. The choice of parallel rack velocities  $V_1$  and  $V_2$  (rather than opposite) frustrates the system, which is only possible because of the noncontact design. The pinion velocity  $V_P$  is taken as positive if it is in the direction shown, as a convention.

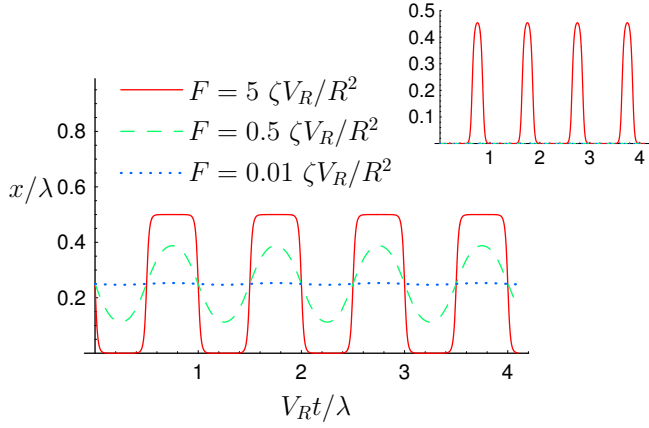


FIG. 2: (Color online). Displacement of the pinion cogs as a function of time [from Eq. (2)] for the fully symmetric device, and  $x_0 = 0.25\lambda$ . For high values of the grip, the motion resembles a square-wave pattern. Inset: the same (three) plots for  $x_0 = 0.0001\lambda$ .

$F \sin[2\pi(x - y)/\lambda]$  from each of the racks, where  $x$  and  $y$  represent the lateral positioning of the surfaces and  $\lambda$  is the wavelength of the corrugations (see Fig. 1), which must be the same on all three surfaces so that coherent coupling is possible. The amplitude of the lateral Casimir force, or the “Casimir grip,”  $F$  depends on the geometric characteristics of the device and in particular the gap size  $H$  and the amplitudes of corrugations.<sup>11,12,13,15,16</sup> These forces add up to exert a net torque of  $-RF_1 \sin[2\pi(x - y_1)/\lambda] - RF_2 \sin[2\pi(x + y_2)/\lambda]$  on the pinion, which should be balanced against the friction torque to obtain the equation of motion for  $x = R\theta$ , where  $\theta$  is the angle of rotation and  $R$  is the radius of the pinion. Putting  $y_1 = V_1 t$  and  $y_2 = V_2 t$ , the equation of motion reads

$$\frac{\zeta}{R^2} \frac{dx}{dt} = -F_1 \sin\left[\frac{2\pi(x - V_1 t)}{\lambda}\right] - F_2 \sin\left[\frac{2\pi(x + V_2 t)}{\lambda}\right], \quad (1)$$

where  $\zeta$  is the rotational friction coefficient.

Equation (1) is symmetric under the combined transformation of  $V_1 \leftrightarrow V_2$ ,  $F_1 \leftrightarrow F_2$ , and  $x \leftrightarrow -x$ . In the fully symmetric case of  $V_R \equiv V_1 = V_2$  and  $F \equiv F_1 = F_2$ , the pinion cannot choose a sense of rotation over the other and performs an oscillatory motion. In this case, Eq. (1) can be solved analytically to yield

$$x = \frac{\lambda}{\pi} \tan^{-1} \left\{ \tan\left(\frac{\pi x_0}{\lambda}\right) \exp\left[-\frac{2R^2 F}{\zeta V_R} \sin\left(\frac{2\pi V_R t}{\lambda}\right)\right] \right\}, \quad (2)$$

where  $x_0$  is the initial position of the pinion. Note that the sign of  $x_0$  determines the sign of the whole solution  $x(t)$ . Equation (2) is plotted in Fig. 2 for different values of the Casimir grip  $F$  and the initial pinion position. It shows that the device can generate interesting periodic patterns such as a nearly perfect square wave or a train of spikes, with a frequency  $f = V_R/\lambda$  that can be

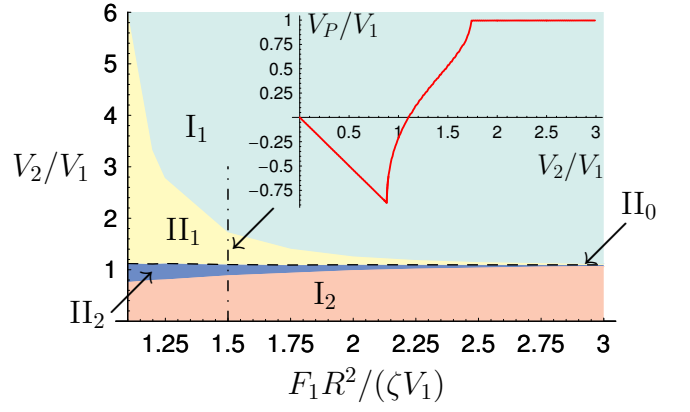


FIG. 3: (Color online). Phase diagram for the motion of the pinion, corresponding to  $F_2 = F_1 + 0.05 \zeta V_1 / R^2$ . There are five different behaviors:  $I_1$  locked with rack-1,  $II_1$  moving with rack-1 with skipping,  $II_0$  neutral oscillatory motion (dashed line),  $II_2$  moving with rack-2 with skipping, and  $I_2$  locked with rack-2. Inset: pinion velocity versus rack velocity for  $F_1 = 1.50 \zeta V_1 / R^2$  and  $F_2 = 1.55 \zeta V_1 / R^2$  (corresponding to a vertical cut of the phase diagram at the dash-dotted line) showing the five different regimes.

easily controlled by the rack velocity. The solution [Eq. (2)] involves an exponential amplification factor that is controlled by the Casimir grip, which could help detect incredibly small displacements. This can be seen in the example plotted in the inset of Fig. 2, which shows a  $10^4$ -fold amplification for  $F = 5 \zeta V_R / R^2$ .

The general form of Eq. (1) allows for richer behavior as the pinion can choose to adopt one net sense of rotation over the other. The pinion can be locked to a rack moving at a given velocity, if the friction force for such velocities can be balanced by the available Casimir grip. This means that the Casimir grips  $F_1$  and  $F_2$  introduce two *skipping* velocities  $V_{S1} \sim F_1 R^2 / \zeta$  and  $V_{S2} \sim F_2 R^2 / \zeta$ , which determine that for  $V_1 < V_{S1}$  and  $V_2 < V_{S2}$  locking of the pinion to the corresponding rack is possible. For larger velocities, the pinion and the corresponding rack will skip cogs.

We have studied the behavior of the device numerically in various parts of the large parameter space of the system. Figure 3 shows a representative phase diagram for a specific section of the space of parameters. It can be seen that the system exhibits five different behaviors ranging from the pinion being locked to rack-1 ( $I_1$ ) or rack-2 ( $I_2$ ) to motion with skipping along rack-1 ( $II_1$ ) or rack-2 ( $II_2$ ). The phase boundary between the two  $II$ -phases (shown in Fig. 3 as a dashed line and denoted as  $II_0$ ) corresponds to the vanishing of the net pinion velocity and thus an oscillatory behavior similar to the symmetric device as described by the solution in Eq. (2) and Fig. 2. Note that the phase boundary between  $I_1$  and  $II_1$  in Fig. 3 is about to asymptote to a vertical line at lower values of  $F_1$  below which the phase  $I_1$  cannot exist (corresponding to  $V_{S1}$  discussed above). The inset of Fig. 3 shows the average pinion velocity for a typical

section of the phase diagram, going from  $V_P = -V_2$  to  $V_P = V_1$  passing through two sharp transition points and zero.

The assumption of a heavily damped system is not unrealistic in view of the technical difficulties of mounting the pinion on an axle or pivot. We can estimate the value of the rotational friction coefficient  $\zeta$  assuming that the main source of friction in the system comes from the lubrication at the axle. For an axle of radius  $r$  which is lubricated with a fluid layer of thickness  $h$  and viscosity  $\eta$ , we find  $\zeta \simeq 2\pi\eta Lr^3/h$  where  $L$  is the thickness (or height) of the pinion. We can also estimate the moment of inertia of the pinion assuming it is a cylinder of mass  $M$  and density  $\rho$ , as  $I = \frac{1}{2}MR^2 = \frac{\pi}{2}\rho LR^4$ . The characteristic time scale that probes the relative importance of inertia and friction is defined as  $\tau = I/\zeta = \rho h R^4/(4\eta r^3)$ . Using  $\rho = 1.17$  gr/cm<sup>3</sup> (for silicone),  $\eta = 10^{-3}$  Pa.s (for a lubricant as thick as water), and the geometrical parameters as  $R = 1$   $\mu$ m,  $L = 10$   $\mu$ m,  $r = 500$  nm, and  $h = 100$  nm, we find  $\tau = 2.3 \times 10^{-7}$  s. For time scales bigger than that, the assumption of a heavily damped system is reasonable.

We can also estimate the skipping velocities using typical values for the Casimir grip, whose value is very sensitive to the gap size.<sup>11,12,13,15,16</sup> For typical (and experimentally realized<sup>17</sup>) values of  $a = 50$  nm (assumed for all surfaces) and  $\lambda = 500$  nm, we find  $F = 0.3$  pN for  $H = 200$  nm that yields a skipping velocity of  $V_S \sim FR^2/\zeta = 3.8$   $\mu$ m/s. However, reducing the gap size (by only a factor of **two**) to  $H = 100$  nm yields  $F = 12$  pN and consequently  $V_S \sim FR^2/\zeta = 150$   $\mu$ m/s (that is enhanced by factor of **forty**). The estimates for

the amplitude  $F$  have been made assuming the boundaries are perfect metals. In practical situations with real metallic boundaries of smaller reflectivity, the Casimir grip tends to be slightly weaker, but the general behavior of the system will still be the same.

The clock signal does not necessarily need to come from the fully symmetric device, and as the phase diagram of Fig. 3 shows it can be obtained by tuning the system into the dashed line ( $\Pi_0$ ) transition boundary for any geometrical design. To get a strong coupling signal like the square wave or the train of spikes shown in Fig. 2, we need to have a rack velocity of say  $V_R = FR^2/(5\zeta)$ , which is equal to 30  $\mu$ m/s for  $H = 100$  nm. This yields  $f = V_R/\lambda = 60$  Hz using the above value for the corrugation wavelength. Higher rack velocities can lead to higher frequencies, although the shape of the signal will change to a simple sinusoidal one as the coupling gets weaker progressively with increasing rack velocity.

In conclusion, we have proposed a design for a mechanical device made of a nanoscale pinion sandwiched without contact between two racks that exert opposing forces, by employing the quantum fluctuations of the electromagnetic field. Because of the frustration that is built into the design, the system can react dramatically to minute changes in the geometrical features in the system and can thus act as a good sensor. The noncontact nature of this device, and other variants based on similar principles, could help us in our quest towards wearproof nanoscale mechanical engineering.

It is a pleasure to acknowledge fruitful discussions with R.A.L. Jones. This work was supported by EPSRC under Grant EP/E024076/1.

---

\* Electronic address: miri@iasbs.ac.ir

† Electronic address: r.golestanian@sheffield.ac.uk

<sup>1</sup> R.W. Carpick, Science **313**, 184 (2006).

<sup>2</sup> M.P. de Boer, T.M. Mayer, MRS Bull. **26**, 302 (2001).

<sup>3</sup> E. Buks and M.L. Roukes, Phys. Rev. B **63**, 033402 (2001).

<sup>4</sup> A. Socoliuc, E. Gnecco, S. Maier, O. Pfeiffer, A. Baratoff, R. Bennewitz, E. Meyer, Science **313**, 207 (2006).

<sup>5</sup> J.Y. Park, D.F. Ogletree, P.A. Thiel, and M. Salmeron, Science **313**, 186 (2006).

<sup>6</sup> H.B.G. Casimir, Proc. K. Ned. Akad. Wet. **51**, 793 (1948).

<sup>7</sup> M. Bordag, U. Mohideen, and V. M. Mostepanenko, Phys. Rep. **353**, 1 (2001).

<sup>8</sup> H.B. Chan, V.A. Aksyuk, R.N. Kleiman, D.J. Bishop and F. Capasso, Science **291**, 1941 (2001).

<sup>9</sup> H.B. Chan, V.A. Aksyuk, R.N. Kleiman, D.J. Bishop and F. Capasso, Phys. Rev. Lett. **87**, 211801 (2001).

<sup>10</sup> R. Golestanian and M. Kardar, Phys. Rev. Lett. **78**, 3421

(1997); Phys. Rev. A **58**, 1713 (1998).

<sup>11</sup> F. Chen, U. Mohideen, G.L. Klimchitskaya, and V.M. Mostepanenko, Phys. Rev. Lett. **88**, 101801 (2002); Phys. Rev. A **66**, 032113 (2002).

<sup>12</sup> A. Ashourvan, M.F. Miri, and R. Golestanian, Phys. Rev. Lett. **98**, 140801 (2007).

<sup>13</sup> A. Ashourvan, M.F. Miri, and R. Golestanian, Phys. Rev. E **75**, 040103 (R) (2007).

<sup>14</sup> T. Emig, Phys. Rev. Lett. **98**, 160801 (2007).

<sup>15</sup> T. Emig, A. Hanke, R. Golestanian, and M. Kardar, Phys. Rev. Lett. **87**, 260402 (2001); Phys. Rev. A **67**, 022114 (2003).

<sup>16</sup> R.B. Rodrigues, P.A. Maia Neto, A. Lambrecht, and S. Reynaud, Phys. Rev. Lett. **96**, 100402 (2006).

<sup>17</sup> U. Mohideen, private communication.